Off-Axis Tensile Properties of γ/γ'-αMo DS Eutectic†

Z. Q. Hu,* J. H. Zhang, Y. B. Xu, Z. Y. Zhang,
Y. S. Zhang, Y. J. Tang

Institute of Metal Research, The Chinese Academy of Science, Shenyang, Liaoning, China

Abstract: This paper reports a study of off-axis tensile properties of γ/γ'-α Mo DS eutectic and the dynamic fracture process directly observed with a scanning electron microscope. If the loading direction deviates from the Mo fiber growth direction, the tensile strength and ductility decrease gradually. During the loading process, two types of cracking are observed: one is cracking of the fiber, and the other is delamination along the fiber-matrix interface. In plastic deformation, slip can pass through both the matrix and the fiber. As a rule, the thicker fibers are cracked earlier than the thinner ones, because they have less defects and better ductility. Delamination is the main source of final fracture.

1 Introduction

After more than two decades of studying directionally solidified eutectics, it is well established that these materials can have excellent high temperature strengths. Many DS eutectics, like the well known γ/γ'-δ and γ/γ'-MC, are composed of a ductile matrix with γ' precipitates and aligned brittle strengthening phases. They possess very high tensile and stress-rupture strengths, but their ductilities are low due to the brittle components. When it is replaced by a ductile one, as in γ/γ'-Mo DS eutectic, its ductility is greatly improved. Such materials are sometimes called second generation high temperature DS eutectics.

Several years ago, Lemkey[1], Henry, Jackson, Walter and Gigliotti[2,3], Sprenger et al.[4] carried out extensive studies on γ/γ'-α Mo DS eutectic, including selection of composition, phase identification, structure, properties, etc. Later, Nakagawa[5] produced DS eutectic by

† 本文原载于《In Situ Composites IV》, 1982, 12: 51~58.
* Z. Q. Hu is now a visiting scientist at M.I.T.

cooling in a fluidized bed. This paper is mainly concerned with the influence of loading direction on the tensile properties of γ/γ'-α Mo DS eutectic, and also the fracture mode.

2 Procedure

Alloy of the desired composition Ni-32.26Mo-6.08Al-1.43V (wt%) was melted in a vacuum induction furnace, cast into rods, surface cleaned and directionally solidified. The temperature gradient was about 100 ℃/cm. The final sample was 80mm long and 26mm in diameter. Growth rates could be varied between 0.5cm/h and 2cm/h, but all the test specimens were all grown with a velocity of 1.5cm/h. The phases and their preferred crystallographic orientation relation-ship were identified by the transmission electron microscope. Dynamic tensile processes were directly observed in a scanning electron microscope.

3 Results and Discussion

3.1 Microstructure

In γ/γ'-α Mo DS eutectic, Mo fibres are square or rectangular in cross section, align themselves parallel to the direction of heat flow, and are enveloped by γ' phase, shown in Fig. 1. There is a strict crystallographic relationship between the orientations of the αMo and γ' phases, viz.

growth direction	$\parallel [001]_{\gamma'} \parallel [001]_{\alpha}$
interface	$(100)_{\gamma'} \parallel (1\bar{1}0)_{\alpha}$

This result is the same as those reported before by Lemkey, Henry et al. Mo fibers become thinner as the growth velocity (R) increases from 0.5cm/h to 2cm/h (shown in Fig. 2). The fiber spacing (λ) obeys the well known equation:

$$\lambda^2 R = \text{constant}$$

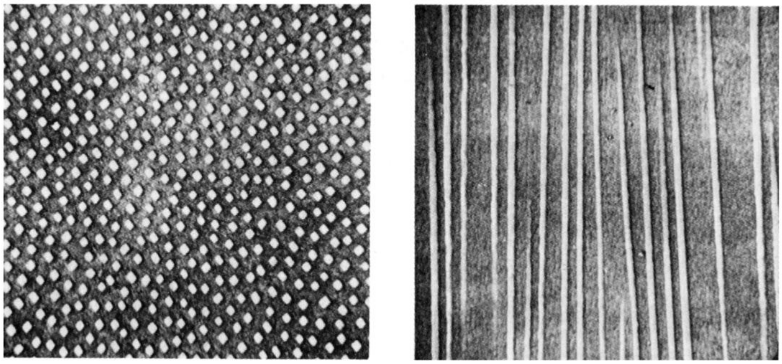

(a) (b)

Fig. 1 Morphology of Mo Fibers
(a) transverse cross section (×1000); (b) longitudinal cross section (×1000)

Fig. 3 shows a linear relationship between fiber spacing and inverse square root of growth velocity of this eutectic.

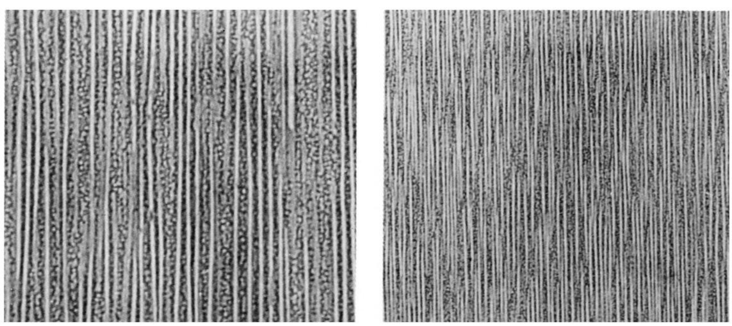

(a) (b)

Fig. 2 Influence of growth velocity on the Mo fiber size
(a) 0.5cm/h (×400); (b) 1.5cm/h (×400)

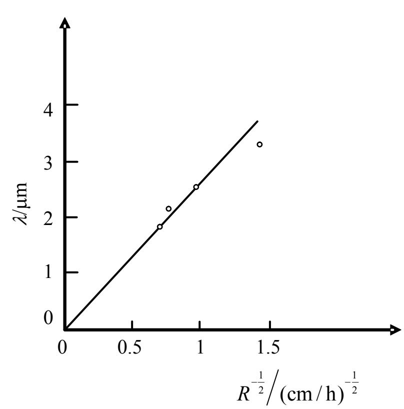

Fig. 3 Relation between growth velocity and fiber spacing

3.2 Mechanical Properties

In order to study the influence of loading direction on the room temperature tensile properties, we chose three angles —0°, 45° and 90°—between the loading direction and the fibber growth direction. Gauge diameter and length were 1.5mm and 7.5mm respectively. Loading speed was 0.3mm/min. Data are listed in Table 1. When the loading direction was parallel to the fibber growth direction, the rupture strength was the highest. The mean value was l359MN/m^2. Rupture strength decreased with the deviation of loading direction from the fibber growth direction. When the loading direction was perpendicular to the fibber growth direction, the rupture strength reached an averaged minimum of 941MN/m^2. The drop was about 31%, but this rupture strength still remained at the level of ordinary cast nickel-base super alloy. Such a lowering of strength is not considered too high. For example, the difference between the transverse and longitudinal tensile strength exceeded 44% for Al-$CuAl_2$, 73C and γ'-δ DS eutectics [6,7]. The tensile ductility of γ/γ'-α Mo DS eutectic is also good, and the elongation perpendicular to the fibber growth direction still remained about 3%. Stress-strain curve under the three conditions mentioned above (see also Table 1) are drawn in Fig. 4(1), (2), and (3) curves represent parallel, 45 degrees and perpendicular conditions respectively. It is clear that curves (1) and (2) show the existence of plastic deformation, while curve (3) reveals no definite evidence for this.

Table 1 Off-axis room temperature tensile properties. asterisks indicate the specimens which stress-strain curves are shown in Fig. 4

Angle	σ_0/(MN/m^2)	δ/%
0°	1392	9.8
	1304	13*
	1382	13
45°	1147	14
	1137	15*
	1078	4.9
90°	965.7	2.9
	975.5	3.0
	901.9	2.8
	921.6	3.1*

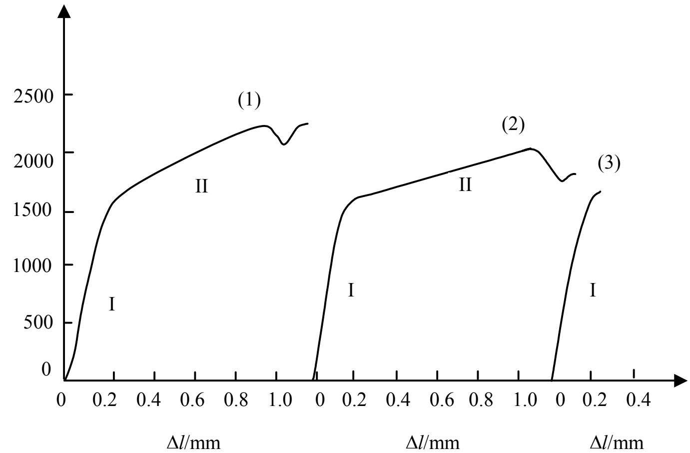

Fig. 4 Room temperature stress-strain curves of γ/γ'-αMo DS eutectic
The loading direction is parallel(1), 45° (2) and perpendicular (3) to the fiber growth direction

3.3 Fracture Process

The dynamic fracture processes of tensile specimens with different loading directions were observed in-situ with the SEM. After the load was applied parallel to the fibber growth direction, elastic deformation began. There was no pronounced change in microstructure (Fig. 5(a)). Continuing to increase the load, plastic deformation took place. The matrix slip system operated, and slip lines cut through the Mo fibres. Slip bands were located about 45 degrees to the fibber growth direction, as shown in Fig. 5(b).

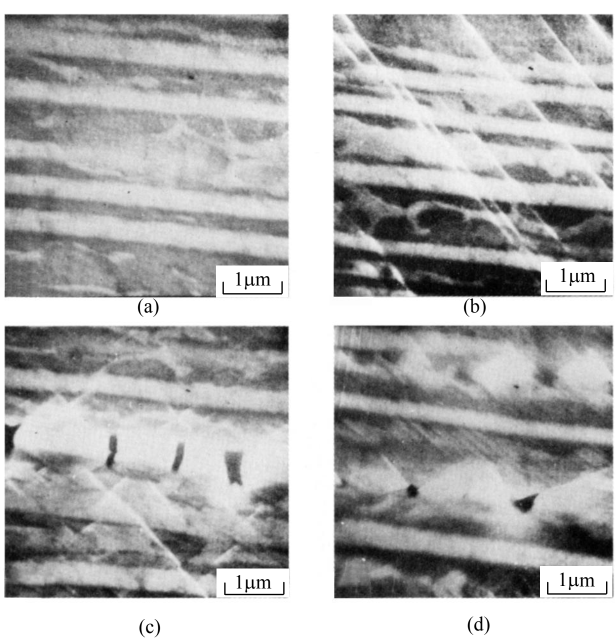

Fig. 5 Deformation process (parallel to the fiber growth direction)

(a) elastic deformation;(b) slip lines cutting through Mo fibers; (c) slip bands intersecting where fibers break into segments; (d) fiber segments shear apart along the slip plane

On increasing the load steadily, we observed two or more slip bands intersecting, where Mo fibres were broken (Fig. 5(c)). Afterwards, gaps between the broken fibres widened and fibre segments sheared apart along the slip plane (Fig. 5(d)).

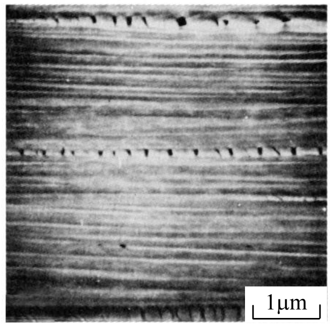

Fig. 6 Thicker fibers first to be broken

Generally, the thicker fibers broke into small segments earlier than the thinner ones (Fig. 6), but that was not the cause of the final rupture. Delaminating along the interface between the fiber and matrix was more important. It propagated and developed into microcracks as the plastic deformation proceeded, as shown in Fig. 7(a). Final fracture was observed in the neck region of the gauge -*a* heavily deformed region (Fig. 7(b)), where the crack changed its propagation direction, turning 90 degrees to its original one. Fig. 7(c) shows the fracture morphology, and Fig. 7(d) is a side view of the fracture surface.

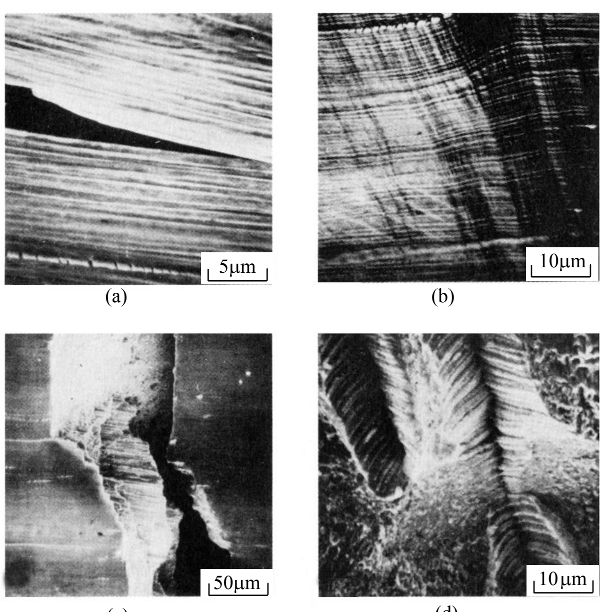

Fig. 7 Fracture process (parallel to the fiber growth direction)
(a) initiation of micro-crack on the interface of fiber; (b) fracture at heavily deformed region; (c) fracture morphology; (d) side view of the fracture surface

If the loading direction was at 45 degrees to the fiber growth direction, fracture proceeded in the same way as before: cutting of slip bands through the fiber (Fig. 8(a)), initiation of delamination, propagation of micro-crack along the interface of fiber and matrix (Fig. 8(b)) and final fracture at the neck region. Fig. 8(c) shows the fracture morphology. It can be clearly seen that the fracture surface is also 45 degrees to the loading direction.

When the loading direction was perpendicular to the fiber growth direction, fracture seemed to be brittle. As soon as the applied load exceeded the limit of elastic deformation, final fracture occurred rapidly. Fig. 9(a) shows the fracture morphology, and Fig. 9(b) shows the fracture surface. It is obvious that fracture appears at the interface of fibers and matrix.

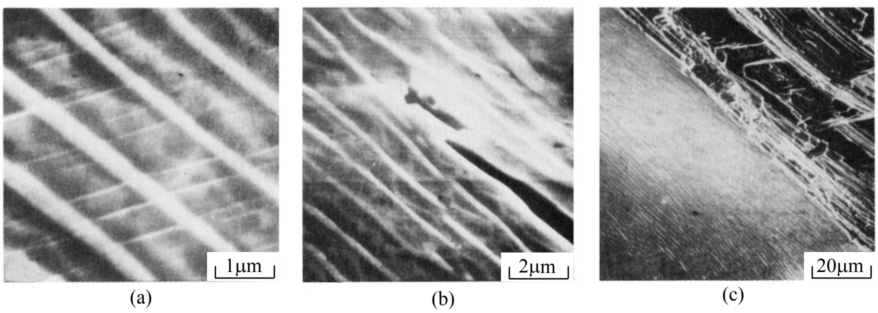

Fig. 8 Fracture process (loading at 45 degrees to the fiber growth direction)
(a) slip line cutting through Mo fibers; (b) micro-crack propagating along the fiber interface; (c) fracture morphology

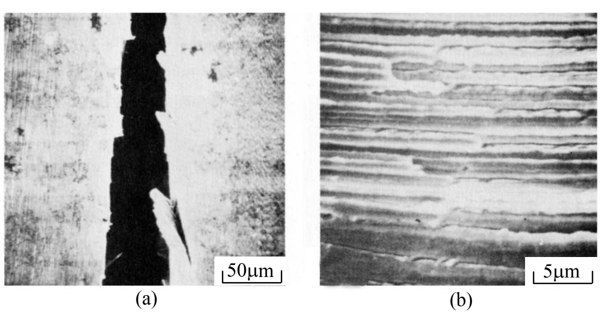

Fig. 9 Fracture process (loading perpendicular to the fiber growth direction)
(a) fracture morphology; (b) fracture surface

All the phases in this DS eutectic are ductile, as can be seen from the microstructure change during deformation process. From Fig. 7(b), one can see Mo fibers deform to a great extent. Face-centered cubic γ, γ' and body-centered cubic α phases have several slip systems. Fig. 10 shows there exist three slip systems at a same moment, with one of them passing through the Mo fibers. The plastic deformation is mainly due to slip. This is why this eutectic is ductile, the room temperature tensile elongation exceeds 10%, if the loading direction is parallel or at 45 degrees to the fibers.

The fracture mechanism can be described as follows: at first it is likely that some of the slip systems may not easily pass through the Mo fiber due to the different structures or orientation, so they are obstructed at the interface, and dislocations pile up there. When these have accumulated sufficiently, delamination initiates, develops and propagates. At the same time, necking occurs, and micro-crack growth accelerates. The crack path immediately changes to the transverse direction at the moment that the specimen cannot withstand the applied load. This explains why the fracture surface is composed of trough-type cracks and many dimples (Fig. 7(d)).

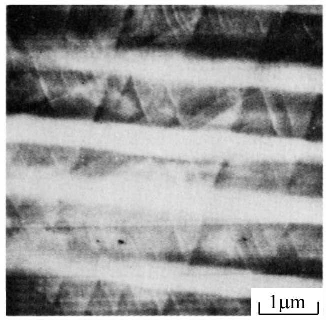

Fig. 10 Slips in γ/γ'-α Mo DS eutectic

Thicker fibers break first. It is probable that they are less perfect than the thinner ones, having more dislocations or other defects, so that the strength and ductility are all worse than the thinner fibers. Because of the ductility of the matrix, cracks in the thicker fibers only grow a bit larger during the deformation process, but do not propagate through the matrix.

When the loading direction is at 45 degrees to the fiber growth direction, the shear stress along the interface of fiber and matrix is highest. Of course, it will produce shear cleavage along the interface.

The final case is when the loading direction is perpendicular to the fiber growth direction. As soon as the applied stress exceeds the strength of the bond between fiber and matrix, the specimen breaks quickly. In this case it is hard to observe any trace of plastic deformation.

4 Conclusion

The microstructure of γ/γ'-α Mo DS eutectic consists of α Mo fibers with square or rectangular cross section aligned parallel in the matrix, The Mo fibers are surrounded by γ' and there is a strict crystallographic orientation relationship between α and γ'.

Two types of cracking are observed during the off-axis dynamic fracture process: cracking of the fiber and delamination along the fiber-matrix inter-face. The thicker fibers break into segments earlier than the thinner ones, but it is not the cause of the final fracture. When the loading direction is parallel or 45° to the fiber growth direction, many intersecting slip bands have been observed. Delamination initiates, develops and propagates at the fiber-matrix interface, that is the main source of final fracture. On the contrary, when the loading direction is perpendicular to the fiber growth direction, the specimen is quickly to be torn apart along the fiber-matrix interface, so its ductility and strength are much lower than the former loading conditions.

5 Acknowledgments

Technical discussions with Professor Chang-Xu Shih, the Institute of Metal Research, Professor M. C. Flemings and M. Simpson, Materials Processing Center, MIT, are gratefully acknowledged. The authors also wish to thank Mr. Y. Yue for assistance with the experimental work.

References

[1] Lemkey F D. Superalloys: metallurgy and manufacture. Proceedings of the Third International Symposium, 1976. 321

[2] Henry M F, Jackson M R, Gigliotti M F X, Nelson P. B. NASA CR-159416, 1979

[3] Henry M F, Jackson M R, Walter J L. NASA CR-135151, 1978

[4] Sprenger H, Richter H, Nick J J I. J. Mater. Sci., 2075

[5] Nakagawa Y G, Ohotomo A, Saiga Y. In "Superalloys", Proc. of the Fourth International Symposium, 1980. 267

[6] Stoloff N S, Duquette D J. *In*: Fractography-Microscopic Cracking Processes. ASTM STP-600, 1975. 154

[7] Stoloff N S. Advances in Composite Materials, 1978. 247

F. D. Lemkey:

During transverse tensile testing was fracture initiated on the γ/γ'-α interface or on eutectic grain boundaries or both?

Author:

Fracture was initiated on the γ/γ'-α interface. Because of limited number of samples we observed, Dr. Lemkey′s suggestion is well worth noticing on our future research work.

M. Thomas:

At 45° one sample had significantly lower ductility than the other two. Is there any explanation for this?

Author:

Data is real but no difference in microstructure observed.